Proceedings of The Institute of Acoustics

SOME PRACTICAL APPLICATIONS OF NONLINEAR ACOUSTICS

Peter J. Westervelt

Department of Physics, Brown University, Providence, RI 02906

INTRODUCTION

I shall discuss the underlying physical principles pertaining to two classes of practical nonlinear acoustical devices. Orifices and spheres are lumped acoustical elements which are the objects of the first half of this paper; continuous or distributed processes involved in the parametric array and the absorption of sound by sound will be taken up in the latter half.

THE THEORY OF NON-STEADY FLOW THROUGH AN ORIFICE.

Introduction

We develop in this section a theory of the response of the orifice (and nozzle) in terms of its steady state behavior. We shall not assume, as did Sivian[1], that the velocity is uniform over the cross section of the orifice, but we will consider the effects of contraction. Losses within the orifice due to friction and turbulence will be lumped together in their effect, and represented by the coefficient of velocity.

The coefficient of contraction is assumed to be a constant. This assumption in addition to the assumption of incompressible flow allows a theoretical expression for non-linear resistance to be derived which can be expressed in terms of the d-c flow resistance.

Next the transmission of sound through an aperture which supports a steady flow of gas is investigated by means of a trivial extension of flow resistance theory. The differential resistance, R_D is introduced as a measure of the acoustic resistance of apertures carrying air flow. The inverse problem, that of the modification of the d-c flow resistance by an intense acoustic wave is mentioned briefly.

The rectifier-like properties of the orifice are considered qualitatively. It is shown that the orifice may be made to support a steady difference in pressure provided it is excited with an asymmetric pressure wave whose square root moment $p|p|^{-1/2}$ differs from zero. This pressure difference can be used to pump fluid through the orifice in a direction which is determined by the sign of $p|p|^{-1/2}$. Harmonic generation by the orifice is discussed briefly. Sivian's prediction of the existence of odd harmonics is reviewed. Second harmonics are shown to be generated by superposed d-c flow.

The Non-Linear Resistance

If the pressure difference across the orifice is less than 1 percent of atmospheric, it is sufficiently accurate to consider the orifice flow to be governed by the equation for incompressible flow. In this the ideal flow equation is:

$$p = p_1 - p_2 = \frac{\rho Q_1^2}{2S^2} \qquad (1)$$

where p_1 is the pressure on the upstream side of the orifice and p_2 that on the downstream side, ρ is the density of the gas, Q is the ideal theoretical volume velocity through the orifice which has a cross section S. Eq. (1) neglects the effects of friction and contraction which will be considered later. If we now assume that Eq. (1) is instantaneously valid, and that p varies sinusoidally, it is a simple matter to compute the average power dissipated. This power divided by one-half the square of the peak volume velocity results in an expression for the non-linear resistance,

$$R_{NL} = \frac{1.1\rho Q}{2S^2} \tag{2}$$

where Q is the peak volume velocity. Eq. (2) may be expressed in terms of u_{rms} the rms average particle velocity through the orifice.

$$R_{NL} = \frac{1.1\rho u_{rms}}{2S} \tag{3}$$

Eq. (2) disagrees by a factor of $1.1/\sqrt{2}$ with the non-linear term in Sivian's equation for resistance which is $1/2(\rho|u|)/s$ and I conclude that sufficient caution was not exercised in its derivation.

Eqs. (2) and (3) could have been derived just as easily from the equation of incompressible flow which has been properly corrected for contraction and losses. This procedure is only valid if the coefficient of discharge C_d is a constant independent of the velocity. Steady flow experiments I have performed justify assuming C_d constant. Inasmuch as the correct flow equation differs from Eq. (1) which neglects contraction by the constant factor C_d^{-2}, we may write immediately the correct expression for the non-linear resistance

$$R_{NL} = \frac{1.1\rho Q}{2(SC_d)^2} \tag{4}$$

The steady flow resistance is

$$R_F = \frac{\rho Q}{2(SC_d)^2} \tag{5}$$

so that we may express the non-linear acoustic resistance in terms of the flow resistance

$$R_{NL} = 1.1\ R_F \tag{6}$$

Eq. (6) will represent the facts if the coefficient discharge has the same value for steady flow as for alternating flow, a situation found not true within the experimentally available frequency range. As will be seen in the following section, the experimental data on thin orifices taken above 200 cps was found to agree fairly well with the relation

$$R_{NL} = .6\ R_F \tag{7}$$

indicating that the a-c flow coefficient is about $(.6)^{-1/2} = 1.3$ times larger than the d-c coefficient.

It is necessary to justify our having neglected the reactance of the orifice in the preceding treatment. This point is considered in more detail in the following section on differential resistance where we shall merely give a physically plausible reason for neglecting reactance. In any event, Ingard and Labate[2] have shown experimentally that the reactance of the orifice decreases appreciably in the region where hydrodynamic laws become applicable.

The Differential Resistance and Reactance

In general, when there is an average transport of matter through a small aperture, the acoustic conductivity of the aperture decreases. This phenomenon can be discussed in terms of the acoustic resistance of the aperture under steady flow conditions; this resistance we shall call the differential acoustic resistance. Strictly speaking it is the complex impedance of the aperture which should be specified. Since, however, even for moderate flow velocities, the impedance of the orifice becomes essentially real, so that the differential resistance is a useful quantity. To see this, we first examine the basic origin of kinetic mass.

The acoustic reactance of a system driven at a single point can be expressed in terms of the time average of L, the Lagrange function for the system evaluated for unit terminal volume velocity amplitude[3]. To a first approximation a small orifice (and the tube to which it is coupled) is a system whose behavior can be expressed in terms of the driving pressure, p, on one side of the orifice and Q, the volume velocity through the orifice. Thus, neglecting interaction between the incident wave and the scattered wave from the orifice, we have for reactance X of the orifice

$$X \approx 4\, j\omega[L_{AV}]_{Q=1} \qquad (8)$$

If all boundaries are rigid, L_{AV} can be expressed in terms of volume integrals of the average kinetic and potential energy densities t_{av} and v_{av}

$$L_{AV} = \int (t_{av} - v_{av})\, d\tau \qquad (9)$$

where the integral extends throughout the region occupied by the field. The reactance of a small orifice in a tube is given approximately by (8) provided the orifice is considered to scatter as a simple source. In this case the integral in Eq. (9) is taken over a spherical volume concentric with the orifice and extending to a radius r_t, where r_t is the radius of the tube. An examination of the integral (9) shows that in the limit when the orifice radius r_t, and for wavelengths long compared with the tube radius, Eq. (9) approaches:

$$L_{AV} \rightarrow T_{AV} \approx (3 + 5)\,\frac{\rho Q_o^2}{48\pi r_o} \qquad (10)$$

The number 3 in the bracket represents the kinetic energy in the region outside the hemispherical caps covering the orifice, while 5 represents the kinetic energy inside.

If a steady stream is superimposed on the sound field, the jet of gas issuing from one side of the orifice will destroy the coherence of the mass contained inside the hemispherical cap on the exit side.

This will remove 1/2 of 5/8 of the kinetic mass of a thin orifice. It is not known how to determine the destroyed fraction of kinetic mass on the inflow side. Assuming for lack of alternative, that the same loss of mass occurs on both sides, we could expect the reactance, under flow conditions to be 3/8 of its normal value. This reduction is in accord with measurements.

We next derive the expression for differential resistance, R_D. This is facilitated by reference to Fig. 1, which serves to summarize compactly the three kinds of resistance, and some approximations involved in their derivation. The pressure-volume velocity curve is drawn assuming a constant coefficient of contraction. If we consider the response to a small signal superposed on a relatively large steady flow, we see the differential resistance is defined to be (just like the dynamic resistance of a vacuum tube) the slope of the p-Q curve at the operating point established by the steady flow velocity. Thus the differential resistance is obtained by differentiating the flow equation (7)

$$R_D = \frac{\partial p}{\partial Q} = \frac{\rho Q^2}{(SC_d)^2} \tag{11}$$

so that we may express the differential acoustic resistance in terms of the flow resistance:

$$R_D = 2\ R_F \tag{12}$$

Eq. (12) will represent the facts if the coefficient of discharge has the same value for steady flow as for pulsating flow. I have verified Eq. (12) experimentally.

A differential flow resistance (not to be confused with the differential acoustic resistance) can be defined which specified the d-c flow resistance of the orifice when an alternating flow is superposed. The problem of modulated flow through an orifice has received some engineering attention because of the errors caused by pulsations in orifice-type flow meters. By straightforward means Lindahl[4] has obtained an expression relating the average flow through an orifice under a pressure head $p = P + \delta p \sin \omega t$ where $\delta p \ll P_o$.

$$Q_{av} = C_d \sqrt{\frac{2P_o}{\rho}} \left[1 - \frac{p^2}{16P_o^2} - \frac{15}{1024}\frac{p^4}{p_o^4}\right] \tag{13}$$

The differential flow resistance is

$$R_{DF} = \frac{P_o}{Q_{AV}}$$

which is, from (12) and remembering that $p \ll P_o$:

$$R_{DF} = \frac{\rho Q^2}{2(SC_d)^2} \left[1 + 1/8\left(\frac{p}{P_o}\right)^2 + \frac{11}{1024}\left(\frac{p}{P_o}\right)^4\right] \tag{14}$$

DEFINITIONS

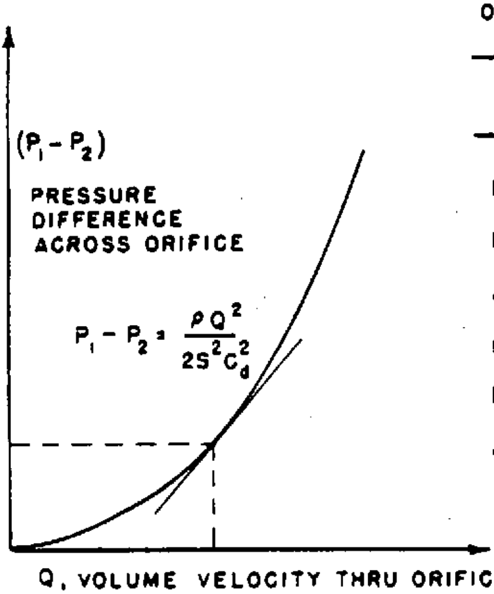

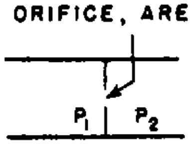

$P_1 = P_0 + \delta p_1$

$P_2 = P_0 + \delta p_2$

$\delta p_2 << \delta p_1 << P_0$

HENCE

$P_1 - P_2 = \delta p_1 - \delta p_2 = p$

∴ TREAT AS INCOMPRESSIBLE FLUID

ANALOGOUS FLOW RESISTANCE : $R_F = \frac{p}{Q} = \frac{\rho Q}{2S^2C_d^2}$

DIFFERENTIAL RESISTANCE : $R_D = \frac{\partial p}{\partial Q} = \frac{\rho Q}{S^2C_d^2} = 2R_F$

NON LINEAR RESISTANCE* : $R_{NL} = \frac{1.1\rho Q}{2S^2C_d^2}$

* NOTE THAT FLOW COEFFICIENTS ARE NOT SIMILAR IN D-C AND A-C CASE

FIG. 1

The bracketed term is obviously a correction factor to the steady flow resistance R_F, which must be applied when there exists a small sinusoidal pressure disturbance.

The Orifice as a Rectifier

The distortion products and steady flow terms produced by an orifice are briefly investigated in this section. We proceed to obtain an expression for the third, and predominant harmonic. Starting from a quadratic pressure-velocity relation $p = KQ^2$, we look for the first two Fourier components of Q when p is sinusoidal. If we say

$$p = P_o \sin \omega t,$$

and $Q = a \sin \omega t + b \sin 3\omega t$

the coefficients a and b are

$$a = \frac{2K^{-1}\sqrt{P_o}}{\pi} \int_o^{\pi} (\sin \omega t)^{3/2} d\omega t = \frac{2K^{-1}\sqrt{P_o}}{\sqrt{\pi}} \frac{\Gamma(5/4)}{\Gamma(7/4)}$$

and

$$b = \frac{2K^{-1}\sqrt{P_o}}{\pi} \int_o^{\pi} \sin 3\omega t (\sin \omega t)^{1/2} d\omega t = 3a - \frac{8K^{-1}\sqrt{P_o}}{\sqrt{\pi}} \frac{\Gamma(9/4)}{\Gamma(11/4)}$$

Thus the ratio of the third harmonic velocity component to the fundamental is

$$\frac{b}{a} = \frac{1}{7} \qquad (15)$$

This is equivalent to a third harmonic that lies 16.92 ≈ 17 db below the fundamental, a result in accord with a certain experiment[5].

The second harmonic component, usually weak in comparison with the third, becomes predominant if a steady flow is superposed on the a-c signal. This is most easily seen by expanding directly the expression for velocity

$$Q = K^{-1}(P_{dc} + P_{ac} \sin \omega t)^{1/2}$$

considering P_{ac} P_{dc}

$$Q = K^{-1}P_{dc}\ 1 + \frac{P_{ac}}{2P_{dc}} \sin \omega t - 1/8\left(\frac{P_{ac}}{P_{dc}}\right)^2 \sin^2 \omega t + 1/16\left(\frac{P_{ac}}{P_{dc}}\right)^3 \sin 3\omega t\ .\ . \qquad (16)$$

From Eq. (16) it is evident that the second harmonic term is greater than the third by a factor of at least P_{ac}/P_{dc}. This effect is easily observed experimentally.

Finally we consider the effect of driving the orifice with an asymmetric wave form such as that depicted in Fig. (2a). While this wave form has a zero average value, its square root moment $p|p|^{-1/2}$ differs from zero as is demonstrated in Fig. (2b). The average volume velocity is proportional to $p|p|^{-1/2}$ so that the orifice is seen to behave as a pump. Experimentally it has been possible to derive enough power from this action to drive a mechanical wet-test flow meter.

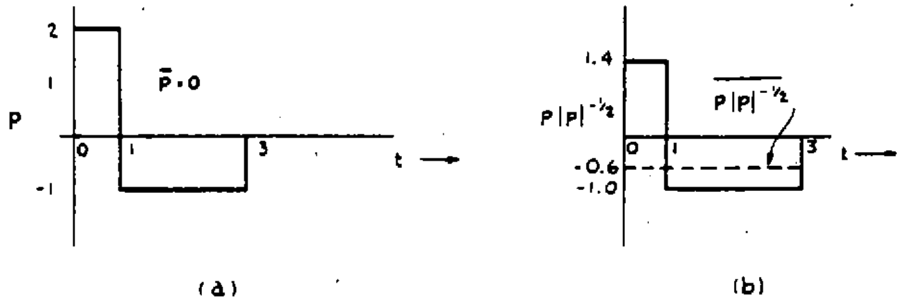

FIG. 2 - A WAVE FORM WITH A SQUARE ROOT TYPE MOMENT

THE ORIFICE--EXPERIMENTAL RESULTS

General Experimental Technique

The orifices studied in this work are small sharp-edged orifices whose diameters are at least two orders of magnitude smaller than the wavelengths of sound used. The principal results were obtained using orifices having diameters of 0.357 cm and 0.5 cm. The range of thickness extended from 0.05 cm to 1.25 cm. The orifices used were also those employed by Ingard[6]. When radius and diameter conform, the orifices used by us are also the same ones that were employed by Bolt, Labate and Ingard[7], as well as by Ingard and Labate[2].

All measurements were performed with the orifice situated axially between two tubes, one having an inner diameter of three inches, the other two inches. Fig. 3 is a block diagram of the principal ingredients of the experiment with the exception of the conventional oscillators, amplifiers, etc. The driving cavity to the left of the orifice was made as small as possible so that high alternating pressures could be generated within by the high powered western electric horn driver unit. The coupling cavity was 2" long with an inside diameter of two inches. The output side of the orifice was coupled by means of a 1-meter long steel tube of 3" inside diameter to a Fiberglas cone whose normal incidence absorption coefficent was 0.99+.

Acoustic resistance was determined by a transmission loss technique. The incident driving pressure was measured by the upstream sound-cell while the a-c volume velocity through the orifice was indirectly determined by the downstream sound cell. The upstream sound cell was placed sufficiently close to the orifice so that no wave correction had to be applied to its readings. Interference from higher order modes was non-existent by virtue of the large values of resistance which were encountered.

Flow resistance was obtained by measuring the time required for a metered quantity of air to flow through the orifice under a fixed pressure head. Within the approximations set forth in Fig. 1, the d-c pressure head is measured by the inclined draft gauge. No static pressure tap was used on the downstream side of the orifice; the orifice was sufficiently small in relation to the tube so that the discharge could be considered to be into atmospheric pressure.

Flow Resistance

It was noticed that the logarithm of the pressure plotted against the logarithm of the volume velocity fell extremely closely on a straight line, provided U, the average particle velocity through the orifice exceeded about 150 cm/sec. Above 150 cm/sec the exponent in the proportionality $p \alpha U^n$ was very close to two as can be seen from the values tabulated below:

diameter cm	thickness cm	n
.357	.09	2.05
.5	.05	1.96
.5	.32	2.10
.5	.64	2.00
.5	1.25	1.96
.5	1.90	1.92
.5	2.54	1.88

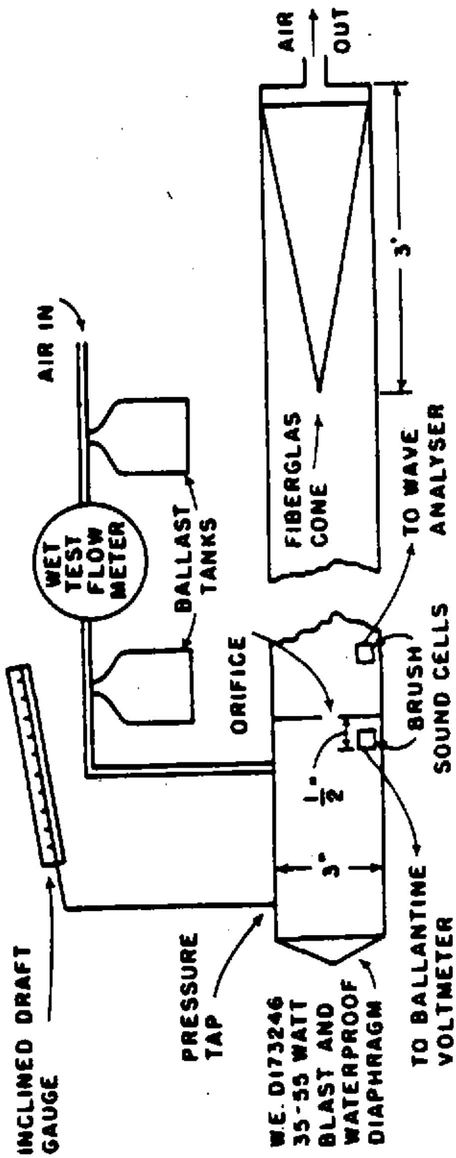
AIR OUT
AIR IN
3'
WET TEST FLOW METER
BALLAST TANKS
FIBERGLAS CONE
TO WAVE ANALYSER
ORIFICE
BRUSH SOUND CELLS
1/2"
3"
INCLINED DRAFT GAUGE
PRESSURE TAP
W.E. D173246 35-55 WATT BLAST AND WATERPROOF DIAPHRAGM
TO BALLANTINE VOLTMETER

FIG. 3

For flow velocities less than 150 cm/sec the log p - log Q relation appears to fluctuate appreciably from a straight line characteristic, a definite tendency to break up being noticed at about 100 cm/sec.

The data have been correlated and expressed in terms of the d-c flow resistance by obtaining the ratio of the pressure to the volume velocity. The data are given in acoustic ohms which have the dimensions of dyne-sec/cm^5 or gm-sec/cm^4.

The measured values of flow resistance are given in Figs. 4 and 5. Plotted for comparison is the value of flow resistance computed from Eq. (7). A discharge coefficient $\frac{1.1}{2}$ = .74 was chosen. This value of the coefficient is roughly consistent with values given in the literature and it enables the flow resistance to be written in a simple way.

For $C = \sqrt{\frac{1.1}{2}}$, $R_F = \frac{1.1\rho Q}{2(SC_d)^2} = \frac{\rho Q}{S^2} = \frac{\rho U}{S}$ (17)

in terms of the average velocity through the orifice U, the orifice are S and the density of air ρ. The measured value of the discharge coefficient is obtained by equating

$$(R_F)_{meas.} = \frac{1.1\rho Q}{2(SC_d)^2}$$

hence

$$C_d = \sqrt{\frac{1.1\rho Q}{(2S^2R_F)_{meas.}}} = .74\sqrt{\frac{\rho v/S}{(R_F)_{meas.}}} \qquad (18)$$

The quantity under the radical is the ratio of the resistance obtained from the heavy curve, $\frac{\rho U}{S}$, divided by the experimental values drawn in lighter lines. Thus the actual coefficient of discharge, evaluated at 500 cm/sec for the thin orifices turns out to be

$C_d = .74\,\frac{2.8}{3.5} = .66$ for the .5 cm orifice

$C_d = .74\,\frac{6.2}{7.9} = .66$ for the .357 cm orifice

A similar computation carried out at 500 cm/sec leads to a value of .87 for both the orifices which are 0.64 cm thick. These larger values of the coefficient obtained for thick orifices result from a decrease in the contraction. A similar computation for the 2.54 cm orifice would indicate that the discharge coefficient for the .5 cm diameter orifice had passed through a maximum, the coefficient now being reduced by the increasing importance of friction in thicker orifices.

<u>The Measurement of Non-Linear Resistance</u>
The transmission loss through a small orifice can be divided into two regions; a low amplitude region in which the transmission loss is independent of the amplitude of the incident sound level and a high amplitude region in which the

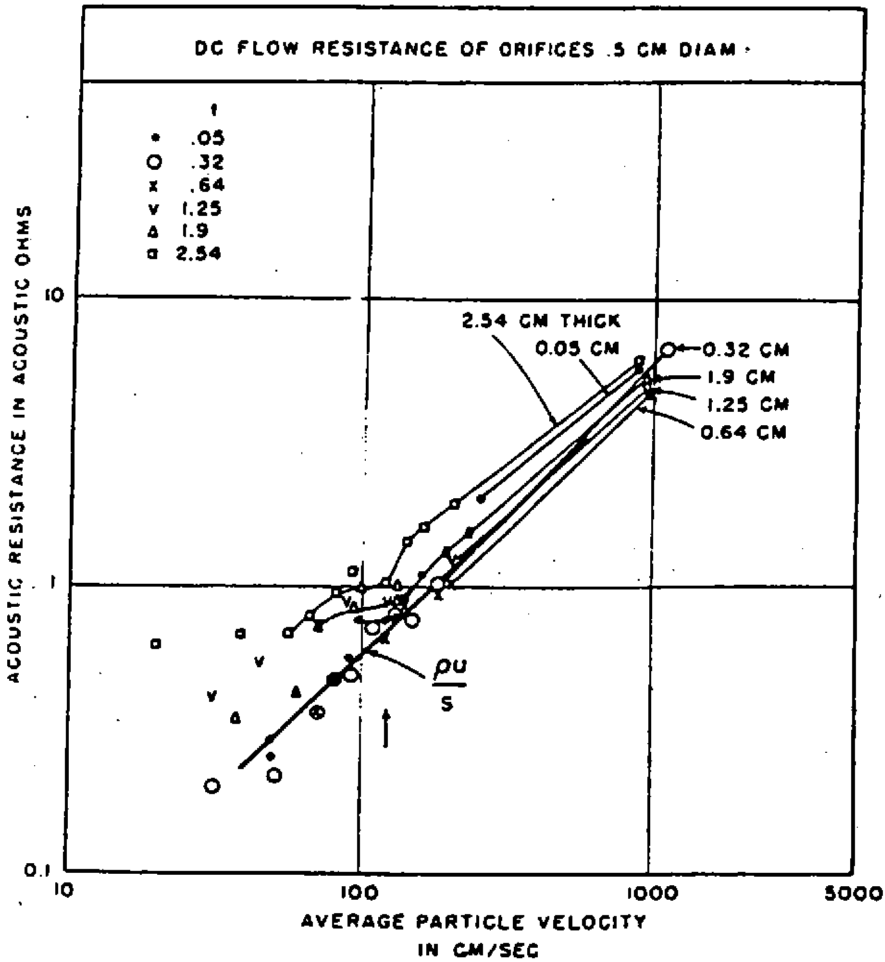
DC FLOW RESISTANCE OF ORIFICES .5 CM DIAM
t
• .05
O .32
x .64
v 1.25
Δ 1.9
□ 2.54
2.54 CM THICK
0.05 CM
0.32 CM
1.9 CM
1.25 CM
0.64 CM
ρu/S
ACOUSTIC RESISTANCE IN ACOUSTIC OHMS
10
1
0.1
10
100
1000
5000
AVERAGE PARTICLE VELOCITY
IN CM/SEC

FIG. 4

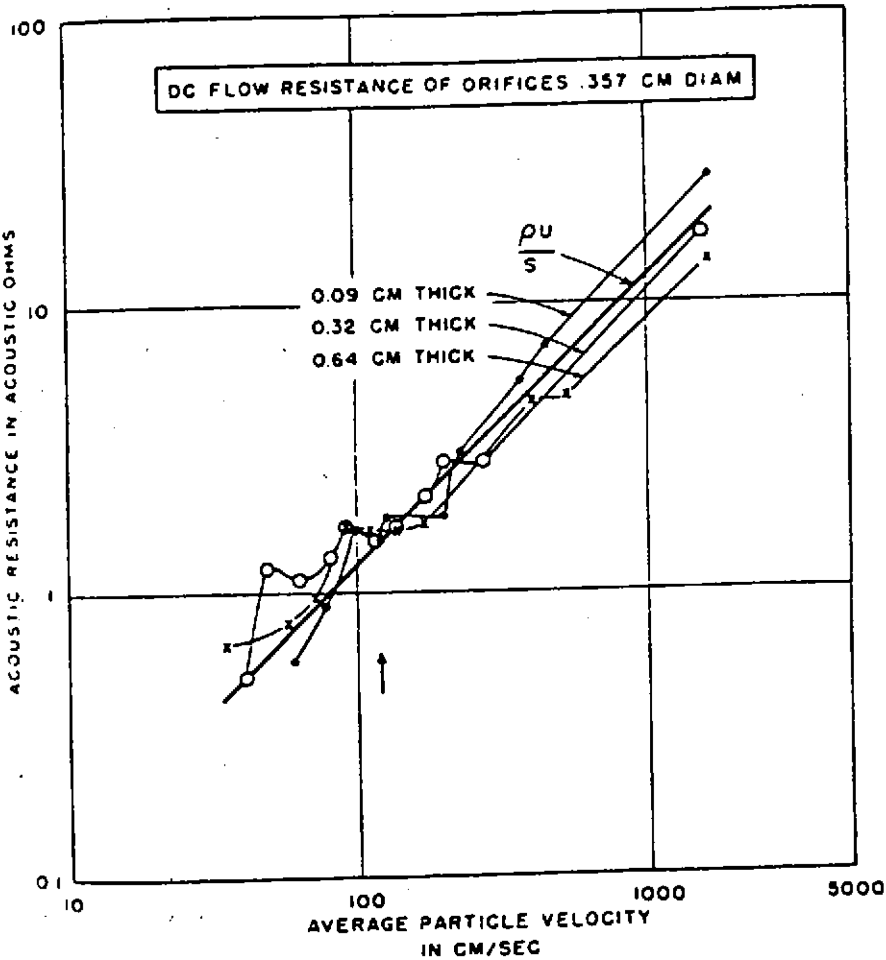
DC FLOW RESISTANCE OF ORIFICES .357 CM DIAM
ρu/S
0.09 CM THICK
0.32 CM THICK
0.64 CM THICK
100
10
1
0.1
ACOUSTIC RESISTANCE IN ACOUSTIC OHMS
10
100
1000
5000
AVERAGE PARTICLE VELOCITY
IN CM/SEC

FIG. 5

transmission loss depends considerably on the incident sound pressure. In the low amplitude, or linear region, the transmission loss is controlled mainly by the mass reactance of the aperture. In the non-linear region the loss is governed by the non-linear resistance of the orifice.

Figure 6 depicts a typical measurement of the sound pressure level transmitted into a three-inch pipe, plotted as a function of the incident sound pressure level. The onset of non-linearity is clearly defined by the abrupt change in the slope of the curves plotted in Fig. 6. In the linear region the slope is 1 db per db; in the non-linear region it is 1/2 db per db. The influence of mass reactance shows up clearly in the linear region of Fig. 6. The transmission loss is seen to increase directly with the frequency at low sound levels. In the non-linear region the curves approach each other and can be represented by a single line. The exact point at which non-linearity sets in is a function both of the frequency and the geometry of the orifice. The critical sound pressure level at which the transmission loss deviates from constancy increases about six db per octave for the orifice of .5 diameter and roughly about 12 db per octave for the .357 cm orifice.

The values of the non-linear resistance obtained by the transmission loss measurement technique are plotted in Figs. 7 and 8. The data are given in acoustic ohms which have the dimensions dyne-sec/cm^5 or gm-sec/cm^4. The data were obtained over a frequency range extending from 150 cps to 800 cps. The non-linear resistance was measured at particle velocity amplitudes between 2000 and 7000 cm/sec; the values plotted have been linearly extrapolated to a particle velocity amplitude of 500 cm/sec.

The resistance appears to increase to its d-c values. It was not possible to determine whether this increase was monotonic as measurements were not obtained at frequencies below the cut-off of the ρc termination.

It is important to emphasize the fact that the values of resistance given in Fig. 7 were not measured at the peak velocity of 500 cm/sec. These data will agree with measurements obtained at 500 cm/sec provided the frequency is low enough to insure that the orifice is in Ingard's jet region.

It is evident that a high degree of correlation exists between the measurements of non-linear and flow resistance. This correlation is even more evident when the two kinds of resistance are plotted for various values of the orifice thickness as is done in Fig. 9. It is particularly clear that the effects of reduced contraction influence the non-linear resistance. According to Eq. (6) the non-linear resistance should be 10 percent greater than the flow resistance provided the same coefficient of discharge is applicable in both cases. It is evident that the non-linear resistance for thin orifices is considerably less than Eq. (6) predicts. This implies that the coefficient of contraction is greater for alternating flow (by about 30 percent) than it is for steady flow. For thicker orifices, the non-linear resistance and the flow resistance are very closely equal. This result agrees with our assumption of a suppressed contraction in the case of orifices whose thickness-to-diameter ratio exceeds about 2.

Measurements of Differential Acoustic Resistance

The differential resistance for two thin orifices of diameter 0.5 and 0.357 cm have been measured by techniques similar to those employed in the previous section. These results are given in Fig. 10 and 11, in terms of acoustic

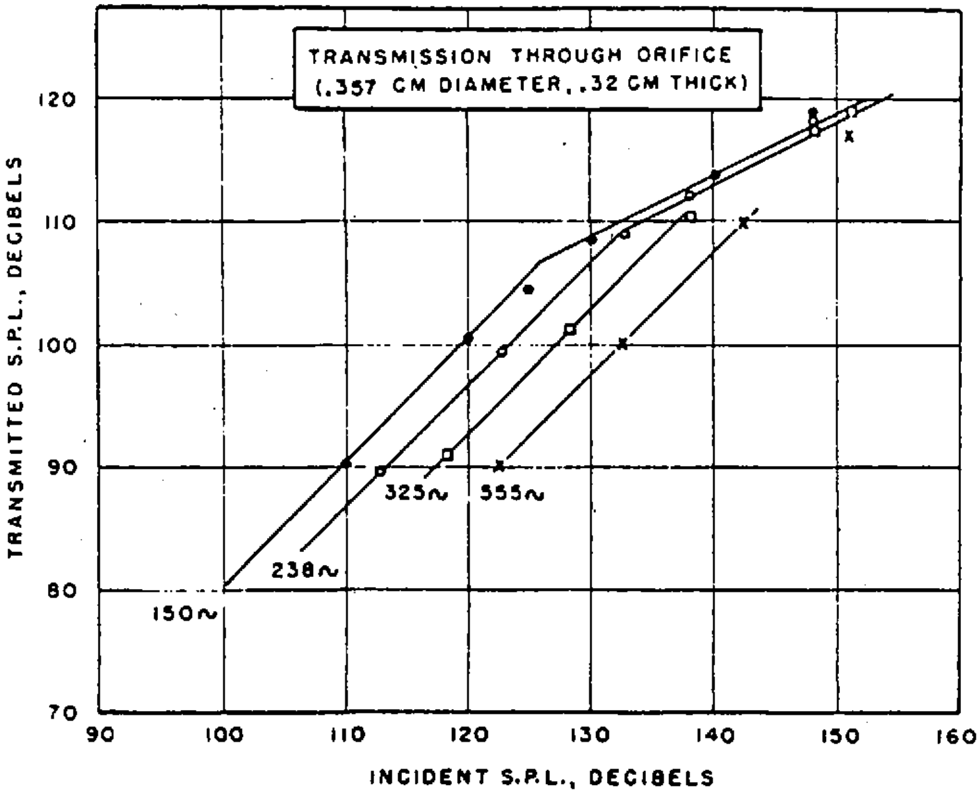
TRANSMISSION THROUGH ORIFICE
(.357 CM DIAMETER, .32 CM THICK)
TRANSMITTED S.P.L., DECIBELS
INCIDENT S.P.L., DECIBELS
150∼
238∼
325∼
555∼
70
80
90
100
110
120
90
100
110
120
130
140
150
160

FIG. 6

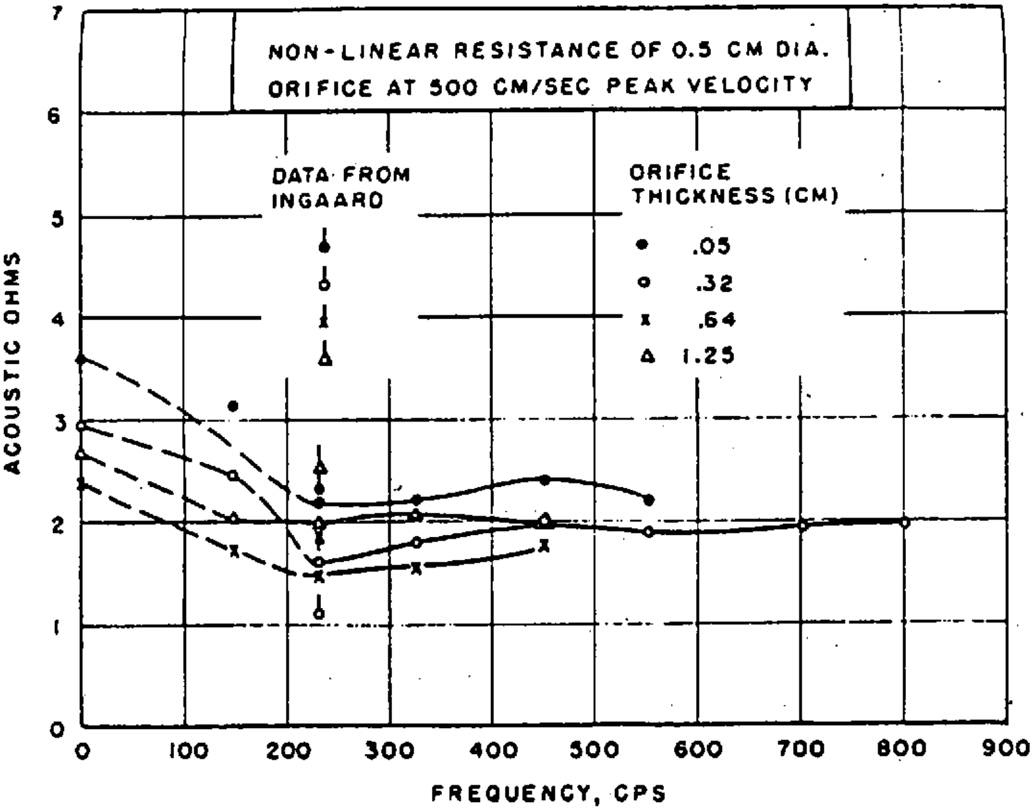
NON-LINEAR RESISTANCE OF 0.5 CM DIA. ORIFICE AT 500 CM/SEC PEAK VELOCITY
DATA FROM INGAARD
ORIFICE THICKNESS (CM)
.05
.32
.64
1.25
ACOUSTIC OHMS
0
1
2
3
4
5
6
7
0
100
200
300
400
500
600
700
800
900
FREQUENCY, CPS

FIG. 7

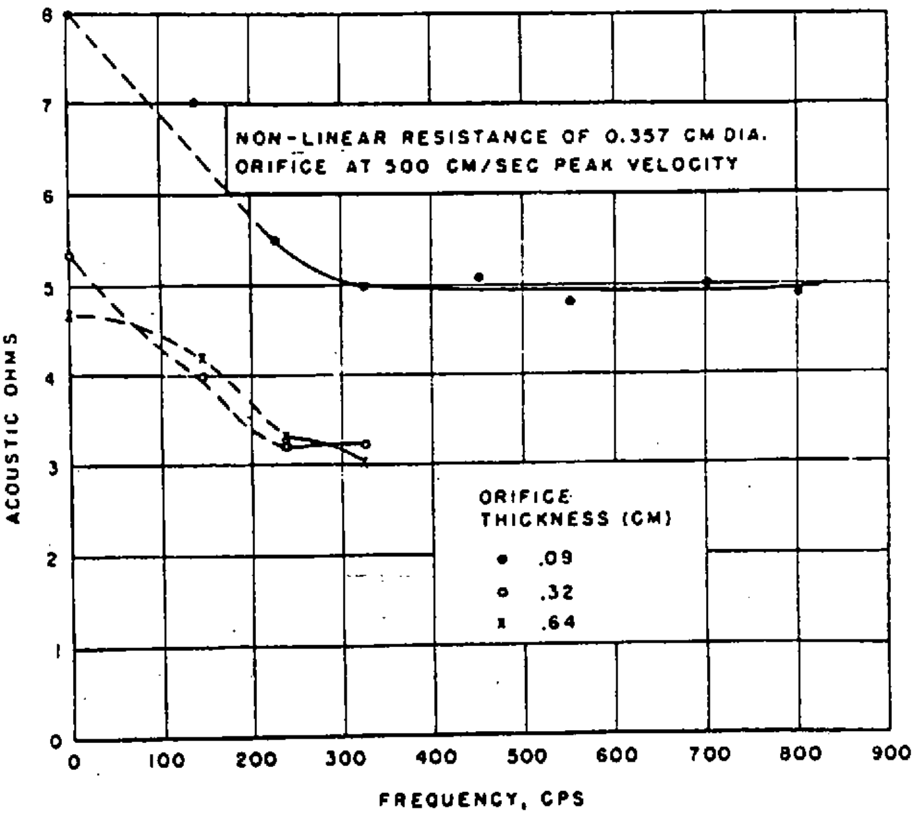
NON-LINEAR RESISTANCE OF 0.357 CM DIA. ORIFICE AT 500 CM/SEC PEAK VELOCITY
ORIFICE THICKNESS (CM)
● .09
o .32
x .64
ACOUSTIC OHMS
0
1
2
3
4
5
6
7
8
0
100
200
300
400
500
600
700
800
900
FREQUENCY, CPS

FIG. 8

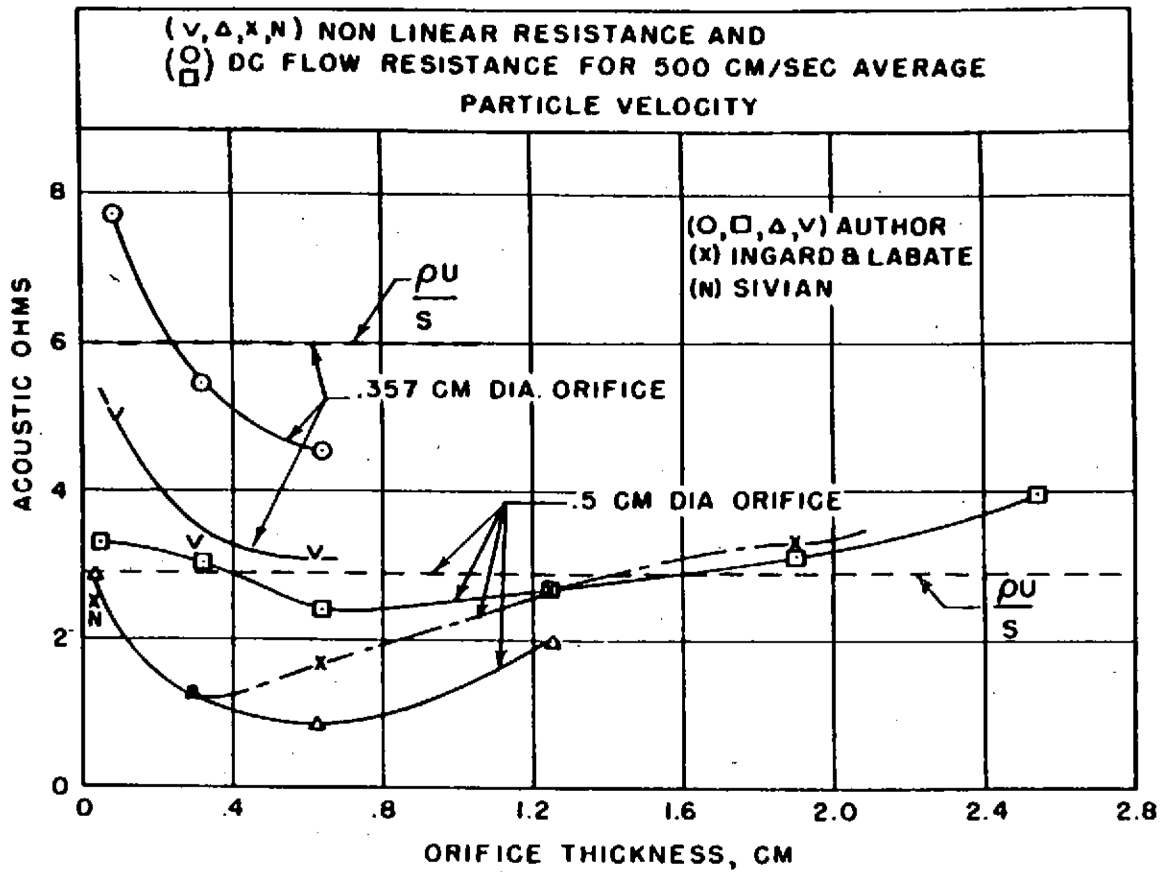
(V, Δ, X, N) NON LINEAR RESISTANCE AND
(O, □) DC FLOW RESISTANCE FOR 500 CM/SEC AVERAGE
PARTICLE VELOCITY
(O, □, Δ, V) AUTHOR
(X) INGARD & LABATE
(N) SIVIAN
ρU/S
.357 CM DIA. ORIFICE
.5 CM DIA ORIFICE
ACOUSTIC OHMS
ORIFICE THICKNESS, CM
0
2
4
6
8
.4
.8
1.2
1.6
2.0
2.4
2.8

FIG. 9

resistance which has the dimensions of dyne-sec/cm^5 or gm-sec/cm^4. The measured values of flow resistance multiplied by 2 are plotted for comparison as well as the equation (11)

$$R_D = \frac{\rho Q^2}{(SC_d)^2} \xrightarrow{C_d = \sqrt{\frac{1.1}{2}}} \frac{2\rho U}{S} \qquad (19)$$

In general the measured differential resistance is less than the flow resistance times 2, and greater than the value calculated directly from the above equation. The measured points corresponding to twice the flow resistance have been omitted from the plot since they would fall on the given solid line. In obtaining the differential resistance, R_D, the a-c velocity amplitude is always considerably less than the superposed d-c particle velocity. As can be seen from Fig. 5, the direction of the d-c flow does not influence the results within the estimated experimental error, which is about 20 percent.

For sufficiently low values of the d-c flow velocity the magnitude of the orifice impedance becomes independent of the d-c velocity. These constant magnitudes of the impedance have been plotted arbitrarily at 100 cm/sec on the abscissas of Figs. 10 and 11. It is of interest to note that for flow velocities of the order of 200 cm/sec the differential resistance is less than the magnitude of the impedance at lower velocities. This means that the acoustic conductance reaches a maximum value and thereafter decreases approximately linearly with a further increase in flow velocity. This behavior may be qualitatively explained in terms of the mass reactance which, for the orifices considered, was greater than the resistance. As the d-c flow increases the coherence of the air mass that contributes to the reactance is destroyed, resulting in a decreased mass reactance and therefore an increased conductance. A further increase in the flow velocity increases the differential resistance so that ultimately the resistance overrides the effect of a reduction in reactance.

The transmission loss technique is inherently incapable of measuring the differential resistance unless this resistance exceeds the magnitude of the reactance. Conversely the reactance may be measured by this method only when its magnitude exceeds that of the resistance. More accurate measurements of the differential resistance and of the dependence of the reactance on flow have subsequently been made by McAuliffe[8] with the precision impedance tube[9]. In Fig. 12 McAuliffe's results for the differential resistance of a .5 cm orifice are compared with our Eq. (19). The reactance is discussed in the following section.

The Influence of Steady Flow and Large Amplitudes on the Reactance

The reactance is observed to decrease considerably with the initial increase in flow velocity. It thereupon levels off to a constant fraction of its former value. It is observed from Fig. 12 that the reactance drops from 26 ohms at zero flow velocity to about 11 ohms at high velocities. This is a fractional reduction in the kinetic mass of 11/26 = .42, which is to be compared with the fraction 5/8 .38, derived from the approximate theory presented in Section II-3.

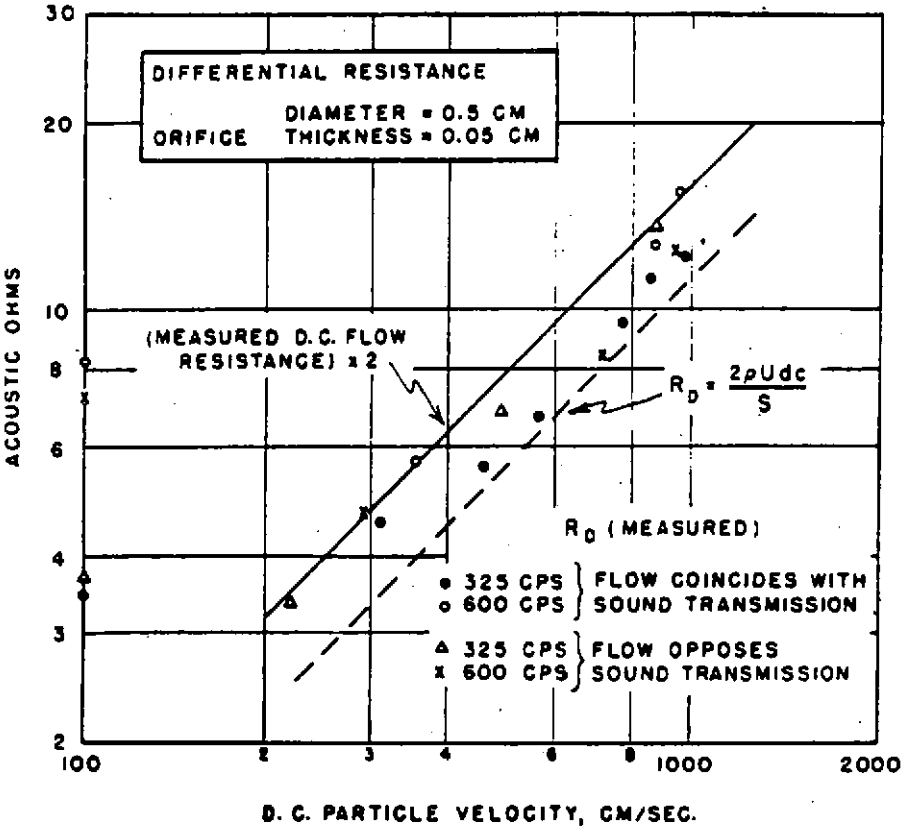
DIFFERENTIAL RESISTANCE
ORIFICE DIAMETER = 0.5 CM
THICKNESS = 0.05 CM
(MEASURED D.C. FLOW RESISTANCE) x 2
$R_D = \frac{2\rho U dc}{S}$
R_D (MEASURED)
● 325 CPS, o 600 CPS: FLOW COINCIDES WITH SOUND TRANSMISSION
△ 325 CPS, x 600 CPS: FLOW OPPOSES SOUND TRANSMISSION
ACOUSTIC OHMS
30
20
10
8
6
4
3
2
100
2
3
4
6
8
1000
2000
D. C. PARTICLE VELOCITY, CM/SEC.

FIG. 10

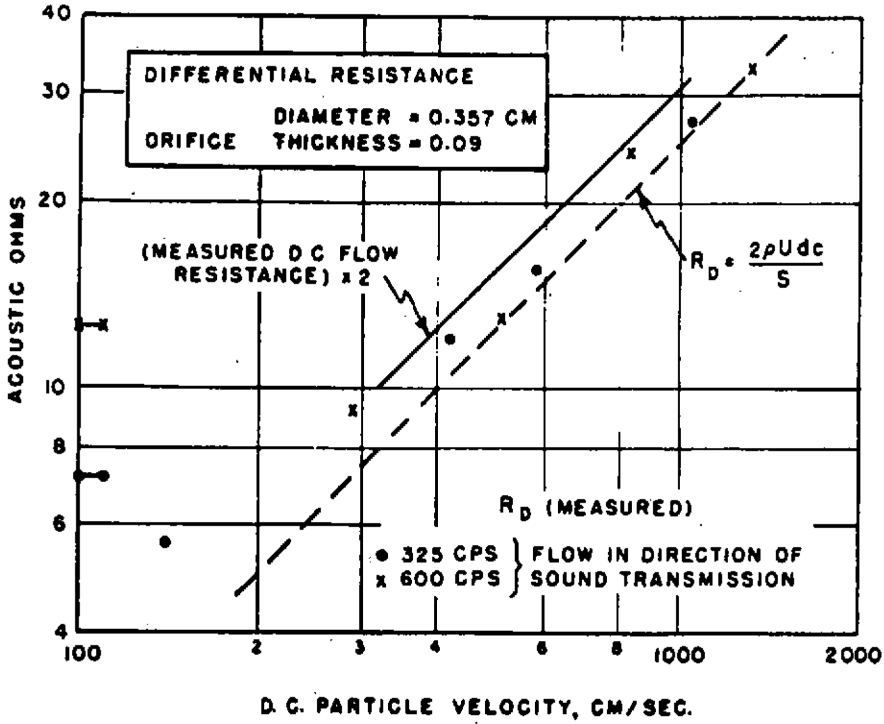
DIFFERENTIAL RESISTANCE
ORIFICE DIAMETER = 0.357 CM
THICKNESS = 0.09
(MEASURED D C FLOW RESISTANCE) x 2
$R_D = \frac{2\rho U dc}{S}$
R_D (MEASURED)
● 325 CPS
x 600 CPS
FLOW IN DIRECTION OF SOUND TRANSMISSION
ACOUSTIC OHMS
40
30
20
10
8
6
4
100
2
3
4
6
8
1000
2000
D. C. PARTICLE VELOCITY, CM/SEC.

FIG. 11

We consider briefly now what we meant in Section II-1 by the statement ". . . the jet of gas issuing from one side of the orifice will destroy the coherence of the mass contained inside the hemispherical cap on the exit side". We adopt the criteria that an element of mass is coherent if it remains within the region bounded by the hemispherical caps on either side of the orifice during one complete period; otherwise it is incoherent. This leads to the following critical relation between the frequency f, the radius r_o and thickness t of the orifice and the maximum flow velocity v_d of the particles:

$$v_c = f(2r_o + t) \tag{20}$$

Applied to the data of Fig. 12 which was obtained at 400 cps, we obtain a critical velocity of 220 cm/sec, which is about one-half the velocity at which the experimentally determined reactance has reached its stable value for high flow velocities. In Fig. 20 this criterion is applied in a slightly different way to the data of Fig. 12 as well as to some additional data. We now use the above concept to estimate the velocity at which a constant non-linear reactance is attained. From considerations similar to those used in the steady flow criterion, we assume the critical particle displacement amplitude in the orifice to be $\xi_c = (2r_o + t)$. Then if u_c is the critical velocity amplitude in the orifice, we have for alternating flow:

$$\xi_c = (2r_o + t)$$

or (21)

$$u_c = 2\pi f(2r_o + t)$$

We apply these last two relations to Ingard's measurements (see Fig. 20) of the non-linear reactance. We note that the reactance of the .357 orifice has stabilized by the time $\xi/t \approx 6$. Since this orifice is .1 cm thick, the critical displacement is 0.6 cm from experiment. From Eq. (4) we find:

$$\xi_c = (.357 + 0.1) \approx .46$$

which is fair agreement.

The Pumping Action of the Orifice

In Section II-4 it was shown that an orifice driven by a pressure wave having a non-zero square root moment should behave like a pump. This behavior was confirmed in a single experiment with the .357 diameter orifice having a thickness of .09 cm. With one obvious exception, the experimental arrangement was equivalent to that utilized in obtaining the differential resistance. Instead of forcing airflow through the orifice, the orifice was called upon to pump air through the flow meter. The required pumping power could be estimated from the product of the pumping rate times the static head which also was measured. The desired waveform was obtained by combining a 600 cps tone with its second harmonic, both having the same sound pressure level, 152 decibels measured behind the orifice. The relative phase between the two waves was adjusted until the maximum pumping rate of .95 liters per minute was achieved against a pressure head of 4" which represents a working rate of the order of one milliwat. The power π dissipated by the orifice can be estimated from the

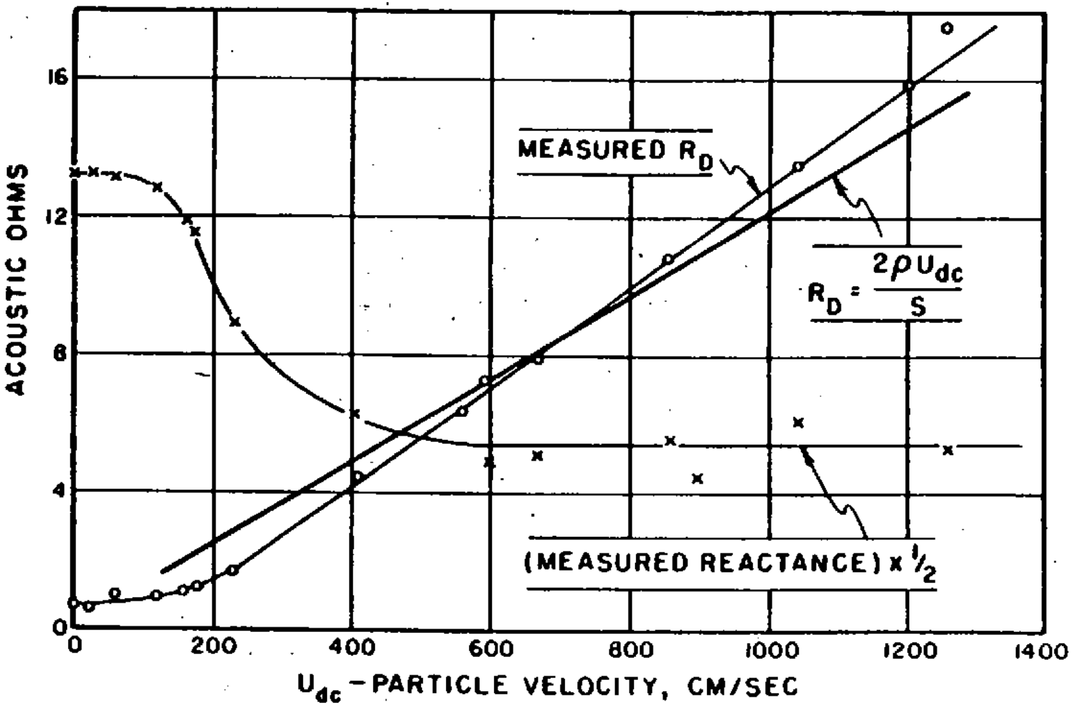

DIFFERENTIAL RESISTANCE AND REACTANCE

ORIFICE DIAMETER = 0.5 CM
THICKNESS = 0.05 CM

FIG. 12

relations

$$\pi = Q_{rms}^2 R_{NL} = \frac{1.1\, Q_{rms}^2 \rho Q_{peak}}{2(C_d S)^2}$$

and

$$\pi = P_{rms} Q_{rms}$$

from which we obtain

$$\pi = \sqrt{\frac{\sqrt{2}}{1.1\rho}}\, C_d S P_{rms}^{3/2}$$

where the symbols have their usual meaning and P_{rms} is the pressure incident on the orifice. Using as an a-c coefficient one that is 30 percent greater than the d-c coefficient we compute that 3 watts is dissipated in the orifice.

The mechanical efficiency of this pump is evidently less than one tenth of 1 percent. Possibly this efficiency could be improved by altering the wave form. Thicker orifices of the same diameter were found to be less efficient pumps.

The fact that small orifices pump quantities of gas has meant that extreme care had to be taken to eliminate small leaks from the tube before valid measurements of the force on objects could be made.

THE THEORY OF STEADY OSEEN FORCES CAUSED BY SOUND WAVES

Introduction

In general sound waves cause steady forces on objects with which the waves interact. The nature of these forces is understood provided one restricts the considerations to ideal fluids lacking viscosity, and heat conductivity. In these cases, if the object is not under steady translation, these forces are due to the well-known radiation pressure.

Consideration is given here to the influence of asymmetry in the velocity wave form of the medium. It is shown that asymmetry in the wave form will give rise to forces, which cannot be explained in terms of the concepts of radiation pressure, but which are caused by the non-ideal nature of real fluids. We have chosen to call the forces arising from asymmetry in the velocity the Oseen-type forces. This has been done in order to emphasize the connection between this force and the force resulting from steady flow which was investigated theoretically by Oseen. The relative order of magnitude of the different forces is depicted in Figure 13 in which r is the radius of the sphere.

The asymmetry in the velocity required to produce Oseen-type forced may be realized in several ways. We have chosen to examine in detail the effects of asymmetry obtained by combining two or more harmonically related waves. The asymmetry which results from endowing either the medium or the particle with a steady velocity in addition to the large amplitude harmonic disturbance is also studied. We have found that these forces which come about through the combined effects of a non-ideal fuid and an asymmetric wave form can be ten or more orders of magnitude greater than radiation pressure.

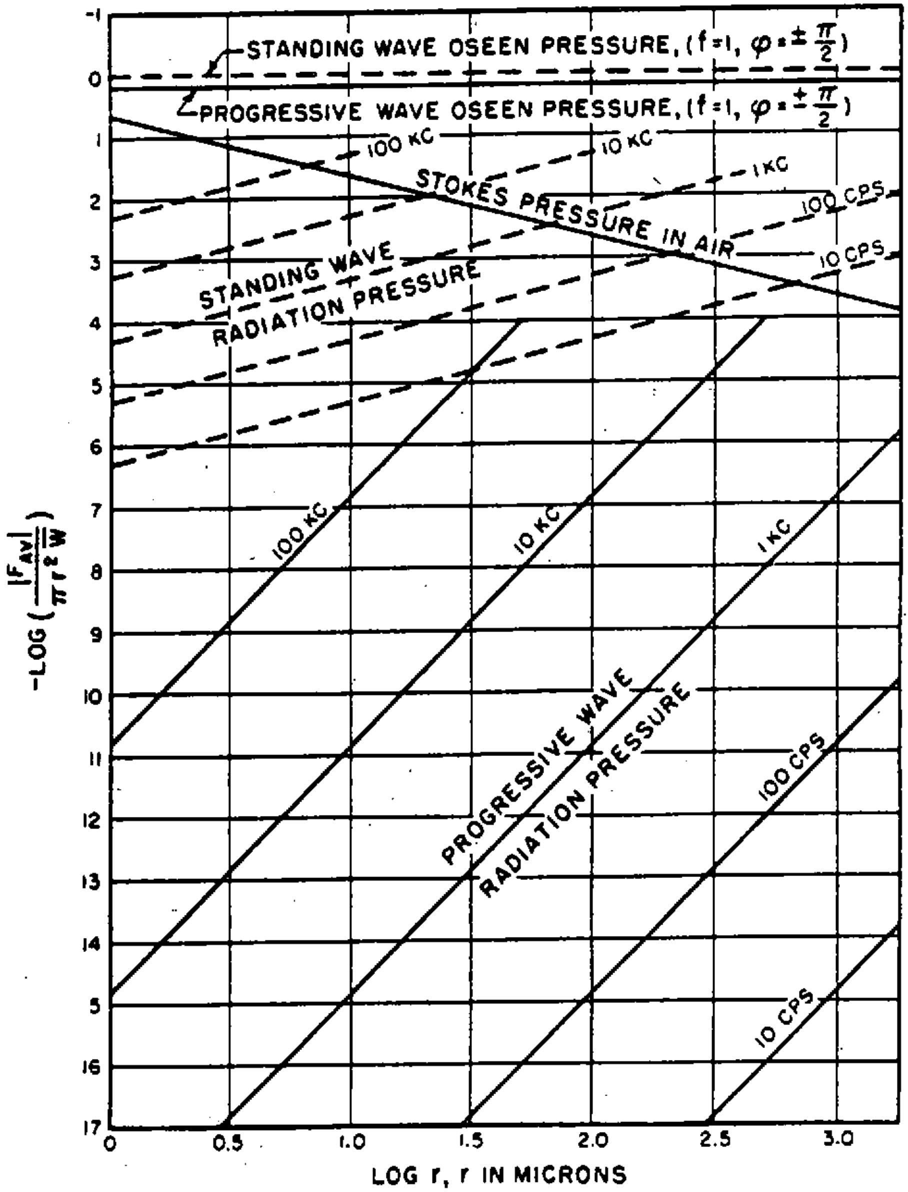

THE PARTIAL DRAG COEFFICIENTS COMPARED

FIG. 13

The non-ideality of the fluid is apparent in the force velocity relation, which is found to exist for bodies undergoing uniform translation. It is well known that an ideal inviscid fluid exerts no force on a body undergoing uniform translation. In a real fluid the force velocity relation is in general non-linear. Hence any treatment which does not take into account the real character of the fluid is apt to lead to unrealistic conclusions.

The Wave Drag Coefficient

In discussing the steady forces caused by sound waves, it has been found expedient to introduce a quantity called the wave drag coefficient and symbolized by D_W. This coefficient is defined as the magnitude of the force per unit local acoustic energy density* divided by the object area projected in the direction of the undisturbed particle velocity. The coefficient D_W may be thought to be the magnitude of the sum of a number of partial vector drag coefficients

$$D_W = \left| \sum_n d_n \right|$$

each d_n representing forces arising from one specific mechanism. The following partial drag coefficients are of interest: d_1, arising from radiation pressure; d_2, involving mean viscous forces; d_3, describing the so-called Oseen-type forces.

In the experiments reported later, the Oseen-type forces are much greater than all the others, so that it is proper to set $D_W = |d_3|$.

The Oseen-Type Forces

The force acting on a sphere moving at a constant velocity relative to a viscous medium can be written to include a term depending on the square of the velocity u:

$$\overrightarrow{\text{Force}} = 6\pi r\, \mu_o \vec{u}\, [1 + k\, |u|\,] \tag{22}$$

where the first term is the well known Stokes law, and the second term involves a constant k that is usually determined experimentally. In steady flow, k is given approximately by Oseen's second approximation to the relation for the drag on a sphere. The relation (22) is usually expressed by giving the hydrodynamic drag coefficient which is defined to be the ratio of the force divided by the projected area of the sphere and the kinetic energy density of the fluid. If C is the drag coefficient then, to within Oseen's approximation, Eq. (22) may be expressed as:

$$C = 24R^{-1} \left\{ 1 + \frac{3R}{16} \right\} = 24R^{-1} + D \tag{23}$$

where R is the Reynold's number for the sphere.

Inasmuch as Oseen's approximation appears to account in a crude way for the facts of steady flow, it is natural to ask to what degree the approximations will hold for non-steady flow. The point of view adopted in this and the

*In some instances we have used twice the average local kinetic energy density in place of the energy density. This allows results obtained in travelling and standing waves to be compared against a common theoretical curve.

succeeding section has been to adopt Oseen's approximation as a point of reference against which experimental results may be compared. In order to carry this program out we first assume Oseen's law to be instantaneously applicable and proceed to derive the consequences of this assumption for non-steady flow.

It may be worth pointing out that for most of the experiments we have done, the objects have been so small and the frequencies so low that the first order acceleration forces are of the same order or smaller than the first order viscous forces. The time average of the first order acceleration force is zero in a periodic wave. We neglect second order acceleration forces. The acceleration forces are tied up with the virtual mass of the sphere. It is possible that the virtual mass is very much reduced under the influence of large alternating amplitudes. This latter point is discussed further in Section 2 of Chapter VII.

It is easy to see that if u is periodic and has a zero average value, the first term in Eq. (12) contributes nothing to the average value of the force. Whether the second term contributes to the average or not depends on whether the average

$$\frac{1}{T}\int_0^T u|u|dt = \overline{u|u|} \tag{24}$$

is different from zero. There is an infinite variety of periodic wave forms which have an Oseen-type moment different from zero. One of the simplest is obtained by combining two harmonically related waves in proper phase as indicated in Fig. 14.

A more general wave than that depicted in Fig. 14 is obtained by considering as adjustable parameters f, the fraction of second harmonic and ϕ, the relative phase angle between the fundamental and second harmonic. Such a wave form would be the following:

$$u = u_o\,[\sin \omega t + f\,\sin(2\omega t + \phi)]$$

It turns out that the normalized Oseen-type moment of this wave can be expressed as the product of two functions

$$\frac{\overline{u|u|}}{u_o^2} = G(f)\Phi(\phi)$$
$$= -G(f)\sin\phi$$

Here G(f) is a function of f along and Φ is a function only of the phase angle.

It is considerably neater to deal directly with the wave drag coefficient, d_3, instead of the force. For this more general wave, then, the coefficient d_3 turns out to be

$$d_3 = \frac{G\Phi}{1 + f^2}\,D = \frac{-4.5\,G\,\sin\,\phi}{1 + f^2} \tag{25}$$

for a plane progressive wave.

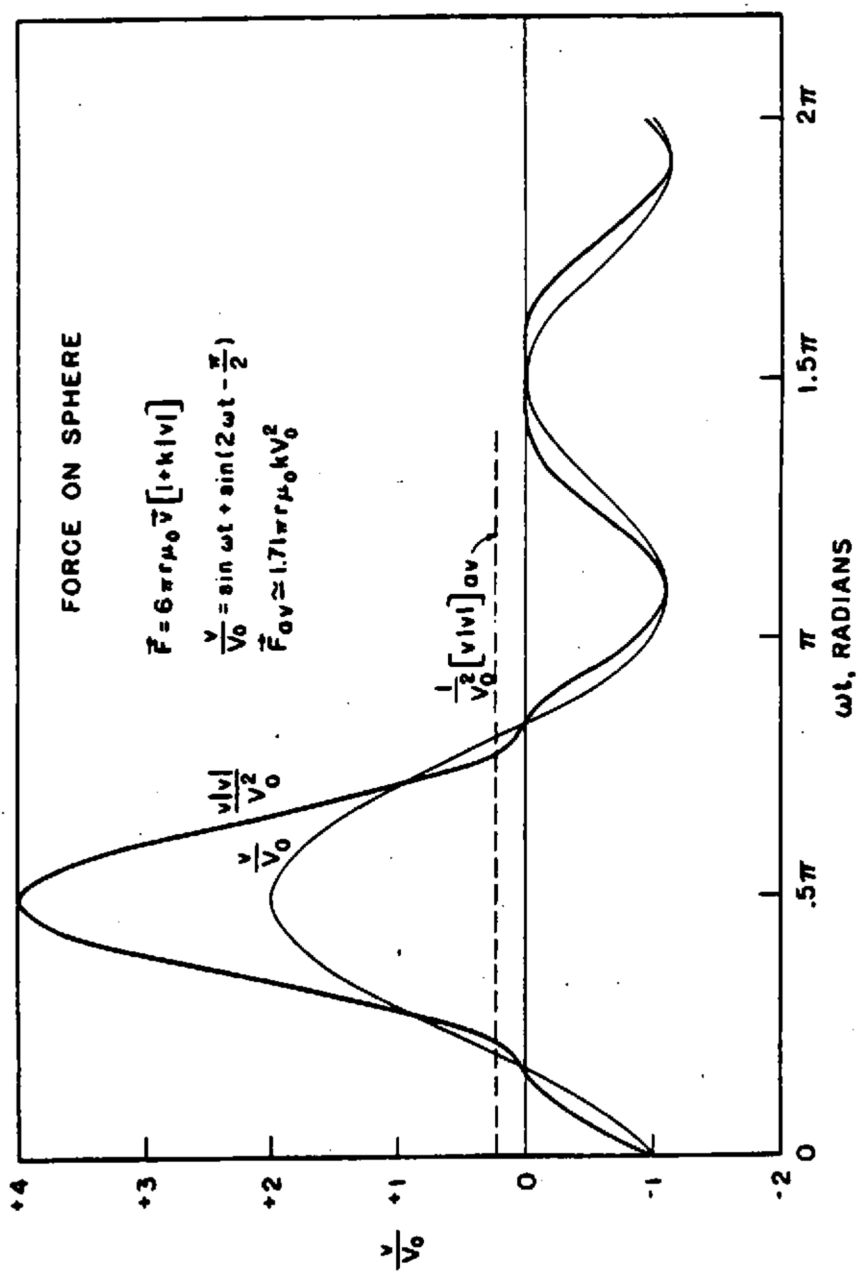

WAVE FORM WITH OSEEN-TYPE MOMENT

FIG. 14

The factor $(1 + f^2)$ in the denominator is proportional to the energy density in the wave. The function G can be shown to be given by the following expression:

$$G = \frac{1}{\pi}\left\{x\sqrt{1 - x^2} + \frac{4}{3}\,fx\,(3 - 2x^2) - f^2\,x\sqrt{1 - x^2}\,[2x^2 - 1] - y(1 + f^2)\right\} \qquad (26)$$

where $x = \cos y$

and

$$y = 1/2\,\cos^{-1}\left[\frac{1}{4f^2}\,(\sqrt{1 + 8f^2} - 1)\right]$$

Approximate and asymptotic expressions for G are easily found to be

$$G \rightarrow \frac{4f}{3\pi} \qquad \text{as } f \rightarrow 0$$

$$G \rightarrow \frac{9\sqrt{3}}{8\pi} - \frac{1}{3} \approx .287 \text{ for } f = 1$$

$$G \rightarrow \frac{1}{\pi} \approx .318 \qquad \text{as } f \rightarrow \infty$$

From these relations we see that the drag coefficient varies inversely with the harmonic fraction, f, for small f, whereas for large f, d_3 varies inversely with the square off. This means that d_3 will have a maximum with respect to f.

Finally we investigate the wave drag coefficient d_3 for a sphere in a moving stream of gas or liquid. The Oseen-type moments have been evaluated for a velocity wave consisting of a constant d-c term in addition to a sinusoidal component. In the event the amplitude of the alternating component is less than the d-c term the velocity may be written

$$u = u_o[1 + f'\sin\omega t] \quad , f' \leq 1 \qquad (28)$$

where f' here indicated the modulation index. The Oseen-type moment of such a wave can be expressed as

$$u|u| = (1 + f'^2/2)u_o^2 \qquad (29)$$

In the event $f' > 1$ we may write for the velocity

$$u = u_o[\sin\omega t + f] \; , \quad f \leq 1 \qquad (30)$$

for which case the Oseen-type moment is shown to be

$$u|u| = \beta(f)\;\; u_o^2 \qquad (31)$$

where $\beta(f) = \frac{1}{\pi}\,[(1 + 2f^2)\,\sin^{-1}f + 3f\,\sqrt{1 - f^2}]$

and $\beta \approx \frac{4f}{\pi}$ for $f \ll 1$,

$\beta(1) = 3/2$

By means of Eq. (29) and the fact that Eq. (28) can be written as

$$u = (f'u_o)\,[1/f' + \sin \omega t],$$

$\beta(f)$ can be defined for any $f \geq 0$.

We are not too much interested in the total force experienced by the object in a combined sonic and flow field. If we were, we would also have to take Stokes' law into account. What we want is the additional force caused by the interaction of the sonic and flow fields. Thus it is necessary to subtract from Eq. (31), f^2, the Oseen moment of the d-c flow field. This leads to a differential β, called β_d and given by:

$$\beta_d = \beta - f^2 \tag{32}$$

from which we can obtain the wave drag coefficient pertaining to a sinusoidal wave in the presence of steady flow:

$$d_3 = C\beta_d = 4.5\beta_d \qquad \text{for } f \leq 1$$

and

$$d_3 = \frac{C}{2} = 2.25 \qquad \text{for } f \geq 1 \tag{33}$$

Thus a d_3 has been found which represents the interaction force per unit project area divided by the acoustic (not including the steady flow kinetic energy) energy density. From Eqs. (33) it is seen that d_3 depends through β_d on the steady flow fraction f provided this fraction is less than unity. If $f > 1$ the drag coefficient is a constant. In the experiments described later the flow velocity was maintained at a fixed value, while f was varied by changing the sound pressure level. In the experiments combining flow and sound the condition $f \ll 1$ was realized so that over the available experimental range

$$d_3 = 4.5\ \beta_d \qquad \text{and } f \ll 1$$

$$\approx 4.5 \qquad \text{by virtue of Eq. (32)}$$

$$\approx \frac{18f}{\pi} \qquad \text{by virtue of Eq. (31)}$$

In Fig. 14 we have compared the three types of forces discussed so far. The charge is primarily intended to convey orders of magnitude and it pertains to spheres and wave numbers for which $kr \ll 1$. Traveling waves as well as standing waves have been treated. The curves for radiation pertain to the classical radiation pressure.